Glioma Modelling Project

Research Thesis

Presented in partial fulfillment of the requirements for graduation *with research distinction* in the undergraduate colleges of The Ohio State University

by

Yolanda Cabello Izquierdo

The Ohio State University

April 2020

Project Advisor: Dr. Jose Javier Otero, Department of Neuropathology

Contents:

Introduction.

Glioma Modelling Project is a tool that could potentially aid any neuropathologist across the world to diagnose brain tumors. According to the World Health Organization (WHO), they're around 200 types of brain and central nervous system tumors. Gender, age, ki-67, general and specific sites are the five parameters that we selected in order to predict brain tumors with an accuracy of sixty percent. This originally created with the idea of saving a patient's money in medical proves. Additionally, there are some countries that do not have access to the same technology or laboratories that, for example, the United States has. Therefore, Glioma Modelling Project could simplify and avoid additive expenses of some laboratory processes that some hospitals do not have.

Tumors that arise in the brain usually involves brain tissue, brain nerve endings, brain membranes, skull bones or skull muscles and are called primary brain tumors. If they extend to other organs of the body, they are classified as metastatic or secondary cerebral tumors. Within primary brain tumors, they can be distinguished between two categories based on the microscopic appearance: benign and malignant. A benign tumor is a tumor that will not spread through the body or invade its surrounding tissue. However, a malignant tumor could potentially invade the surrounding tissue and spread through the body. In addition, primary brain tumors can be categorized as glial (if they are composed of glial cells) or non-glial (if they are developed in brain structures that include nerves, blood vessels as well as glands). Metastatic brain tumors, or secondary cerebral tumors, do not arise in the brain but in other body parts and migrate to the brain, most commonly through the bloodstream (AANS).

There are different types of benign brain tumors such as Chordomas, Craniopharyngiomas, Gangliocytomas, Glomus jugulare, Meningiomas, Pineocytomas, Pituitary adenomas and Schwannomas. Gliomas, Astrocytomas, Ependymomas, Glioblastoma multiforme, Medulloblastoma and Oligodendriogliomas are all malignant brain tumors found, with gliomas being the most common. All of them arise from the glia, which are supporting cells that are subdivided into astrocytes. These star-shaped supporting cells are part of the supportive tissue of the brain. Ependymal cells are thin neuroepithelial lining of the ventricular system of the brain and the central canal of the spinal cord, with oligodendroglial cells providing support and insulation to axons in the CNS (AANS).

The WHO divides brain tumors into four categories according to their growth tendencies and data on histomorphology and molecular status. Tumors that grow slowly are classified as low-grade and can be grades I or II, whereas ones that grow more aggressively are always classified as III or IV high-grade tumors. However, it is very important to understand that all tumors are independent from the grade they are classified as, with all of them being life threatening (AANS).

Grade I tumors are usually the least malignant, typically curable via non-infiltrative surgery, and have long-term survival rates as they are slow growing. Pilocytic astrocytoma, Craniopharyngioma, Glangliocytoma and Ganglioglioma are examples of this classification. Diffuse Astrocytoma, Pineocytoma, and pure oligodendroglioma are Grade II tumors. They're relatively slow growing, somewhat infiltrative surgery and they may recur as a higher grade. Grade III tumors are both malignant and infiltrative and they usually tend to recur as a higher grade. Anaplastic astrocytoma, Anaplastic ependymoma and Anaplastic oligodendroglioma are

found (AANS) in this category. Grade IV tumors are the most malignant. They grow very aggressively, are widely infiltrative, and have a rapid recurrence as well as being prone to necrosis. Glioblastoma multiforme, Pineoblastoma, Medulloblastoma and Ependymoblastoma are the types of tumors that fall within this category. Figure 1 below shows these four categories.

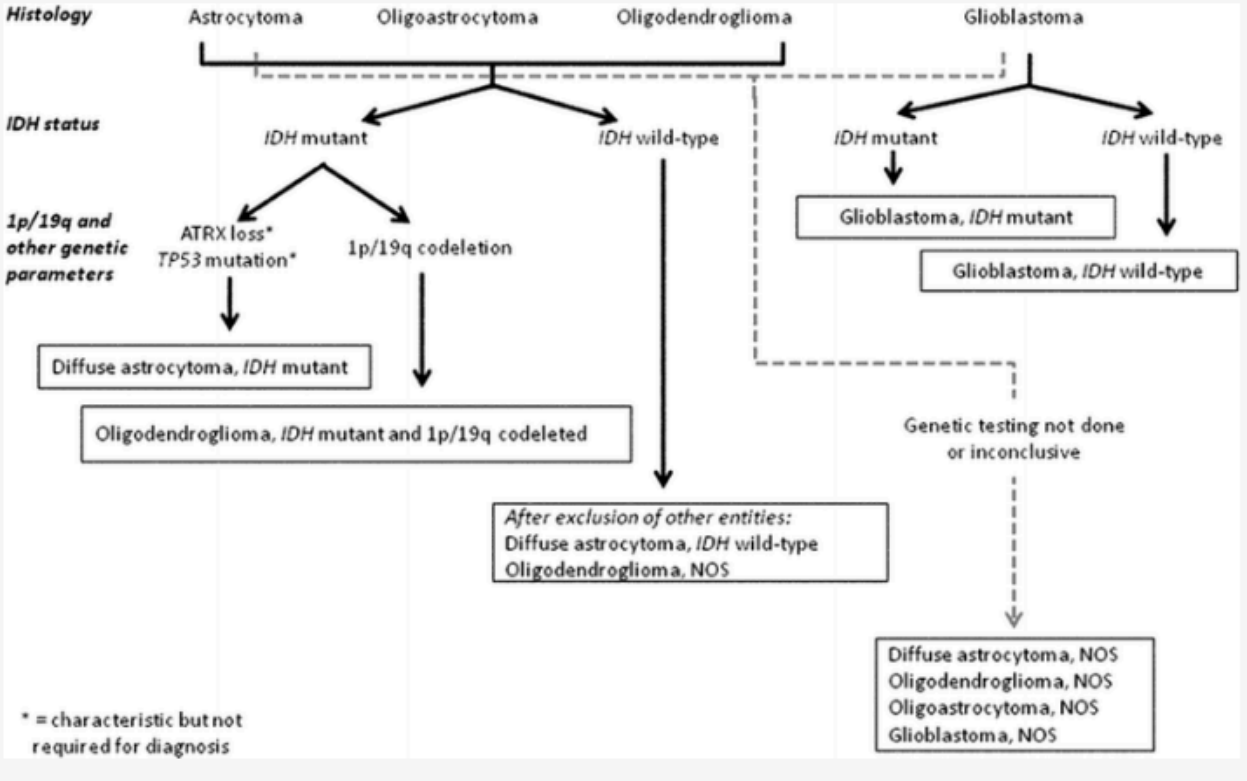

Figure 1. WHO Scheme explains how the tumors are being classified

In 2016, the WHO restructured brain tumor classification by incorporating new entities that included histology and molecular features in their nomenclature. Examples of this are Glioblastoma IDH-wildtype and glioblastoma with IDH-mutant; diffuse midline glioma H_3 K_{27}M-mutant; RELA fusion-positive ependymoma; medulloblastoma with WNT-activated and medulloblastoma SHH-activated; as well as embryonal tumor with multilayered rosettes, and C19MC-altered. The WHO also deleted some entities that are no longer biologically relevant.

For diagnoses closer to 0% malignance, the expected molecular features are IDH mutation, 1p/19q codeletion and TP53 mutation (Pisapia, 2017). IDH1 is a gene that encodes a metabolic enzyme named isocitrate dehydrogenase 1. This enzyme catalyzes the conversion of isocitrate to alpha-ketoglutarate. The mutation of this gene predicts longer survival. Methylated MGMT is an inactive gene that also predicts a longer length of survival. 1p19q codeletion is the combination of a complete loss of the short arm chromosome 1 and the long arm of chromosome 19. This marker usually encodes for a better prognosis (Muzio et al.). EGFR mutation has a high level of cytokines that usually activates gp130 and leads to cell proliferation (Olar et al., 2014). The features that distinguish glioblastomas from other diagnoses are the appearance of dead cells or necrosis as well as the increase of blood vessel growth around the tumor (ABTA). Glioblastomas can be divided into: Glioblastoma IDH-wildtype and IDH-mutant.

Glioblastoma IDH-wiltype, are most commonly found within the temporal lobe (in 31% of the cases), the parietal lobe (in 24%) and in the frontal lobe (in 23%) (WHO, 2016). Predominantly found within patients around 55 years of age (ABTA), this type of tumor will most likely include positive ATRX as well as IDH1 and p53 (Pisapia, 2017).

For glioblastoma IDH-mutant, it is predominetly found within the frontal lobe (WHO, 2016). The IDH-mutant is usually found in patients around 45 years old (ABTA). This tumor is positive for IDH1 mutation as well as ATRX (indicating intact expression) and commonly shows a wild-type pattern for p53 expression (Pisapia, 2017).

In order to compare and constrast how molecular and clinical features differ within tumors, a subtype of oligodendroglioma, meningiomas and astrocytic tumors will be explored in detail.

In oligodendroglioma IDH-mutant and 1p/19q-codeleted the most common location, accounting for more than 50%, is the frontal lobe followed by the temporal, parietal and occipital, respectively. The involvement of more than one cerebral lobe is not common (WHO, 2016). The common age range for this diagnosis is between 35 to 44 years, and ~~i~~s rare when found in patients younger than 16 (Martinez-Larger et all, 2019). IDH1 as well as 1p/19q co-deletion is found within this tumor type.

Pleomorphic xanthoastrocytoma is often found within the supratentorial region, most commonly in the frontal lobe (WHO, 2016). The mean age is aroud 18 years. Necrosis is usually not presented as well as IDH mutation. BRAF V600E is often mutated. The combination of BRAF V600E mutation with an absence of IDH mutation supports the pleomorphic xanthoastrocytoma diagnosis (WHO, 2016).

The majority of meningiomas arise in intracranial, intraspinal or obital locations (WHO, 2016). This tumor it is not aplicable for 1p/19q neither IDH1 and IDH2 mutations (WHO, 2016).

Machine learning is an application of automatic artificial intelligence that has the capacity to automatically learn and improve from experience without being programmed by their provided systems. It is focused on the progress of computer programs and data access (Expert System, 2019). There are two major types of machine learning algorithms: supervised machine learning algorithms and unsupervised machine learning algorithms:

Supervised machine learning algorithms can predict future events based on applying what they already know from the past to new data using tagged examples. From a known data training dataset, supervised machine learning creates a certain function that make predictions about the possible output values. This, can also contrast the calculated output with the correct one in order to find errors that could modify the model (Expert System, 2019).

Unsupervised machine learning algorithms are used when there is no necessity to classify or label certain information. Thus, it can infer a function to describe a hidden structure from no labeled data. The main advantage of this algorithm is that it examines the given data and can show inferences from datasets in order to depict hidden structures from unlabeled data. Also, this algorithm usually does not calculate the right output (Expert System, 2019).

Confusion matrix or error matrix solves the problem of statistical classification. It is the total results of predictions of a determined classification problem. The main point of the confusion matrix, is the summation of the correct and incorrect predictions with count values and broken down by each class showing which parts of the model are causing that confusion, while assessing what type of errors are being made (GeeksforGeeks, 2018).

Decision trees were the algorithms used to predict the possibilities of diagnosis at the highest accuracy. A decision tree can complete classification as well as regression tasks of complex datasets. The algorithms are used in order to construct our model were Random Forest, Boruta, XGBoost and C5.0.

Methods.

1. ***"La Tabla"***

In order to organize the different tumor types, the most updated version of the WHO Classification of Tumors of the Central Nervous System in 2016, was taken to set up a Microsoft Excel table called “La Tabla” that contained all the tumor types in the y axis. All the tumor types were carefully distributed according to specific age of diagnosis onset, e.g. Figure 2.

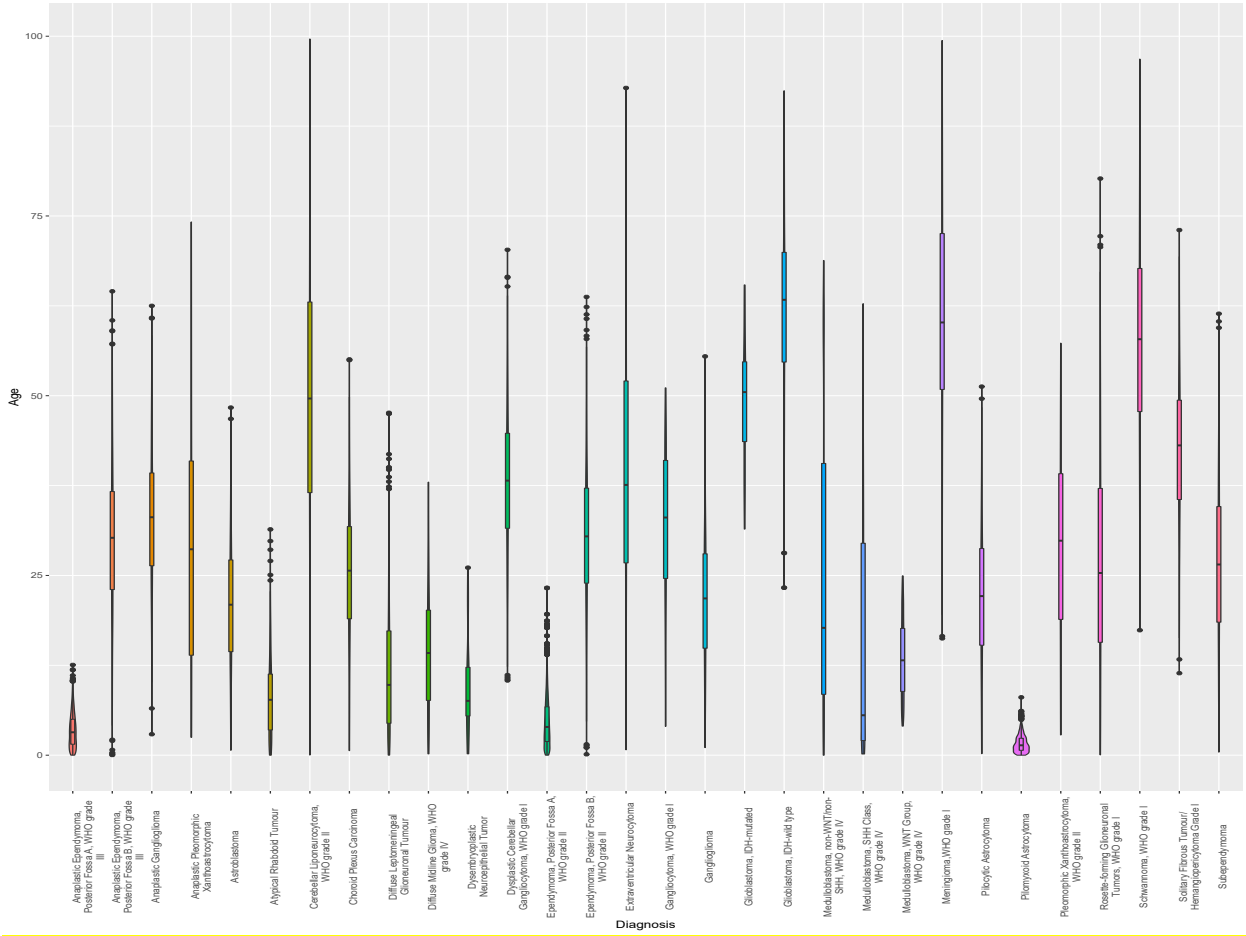

Figure 2. Distribution of tumor types based on mean age of diagnosis.

The x axis is composed of the tumor type, cell type, epidemiological features linked to frequency, mean age, SD of mean age, median age, SD of median age, range age, gender ratio, anatomical sites, global cellularity, pattern of growth, architectural pattern, type of cells

according to frequency, nuclear pleomorphism, additional features, referred to Ann-Mayo classification immunohistochemistry, molecular data and references.

Some of the x-axis labels are subdivided into different categories: Global cellularity is subdivided between low cellularity, medium cellularity and high cellularity. Pattern of growth is split in to infiltrative diffuse and solid with infiltration. Architectural pattern is divided in to nodular (nests), solid discohesive, cords or columns, chicken-wire, pseudopapillary, mycrocystic, myxoid areas, perivascular pseudorosettes, multilayered rosettes, storiform and desmoplasia. Type of cells according to frequency is subcategorized in to astrocytic like (fibrillary, gemistocytic, piloid), resemble subependymal glia (including physal-cells), rounded cells with clear halo (including neurocytic cells), gigant multinucleated cells, rabdohid cells (cells with large eosinophilic cytoplasm, with rounded nuclei with prominent nucleoli), ganglion cells (large cells, with only one nuclei, usually euchromatic), lipidized cells (includes multivacuolated and focal accumulation of lipid-laiden cells), small rounded blue cells and epitheloid cells. Low, medium and high nuclear pleomorphism fall within the nuclear pleomorphism's category. In some additional features dysplastic neurons (neurons that look like mature neurons but are binucleated), rosental fibers, eosinophil granular bodies, perivascular lymphocytes as well as calcifications are found. Referred to Ann-Mayo classification is divided in to, mitosis, endothelial proliferation and necrosis. Immunohistochemistry is subdivided between GFAP, ATRX loos, p53, IDH1 R123H, INI1 (loss stain) and ki67. Finally, molecular data is divided in to the presence or absence of IDH1 and IDH2 mutation, EGFR amplification, MGMT promoter methylation, BRAF V600E mutation, 1p/19q codelection FISH and 1p/19q codelection LOH.

The majority of the information was found within the 2007 and 2016 version of the WHO Classification of Tumours of the Central Nervous System. The rest of the information was reached from scholar articles as well as neurophatology and neuro-oncology literature.

Tables 1 and 2 include the information that we got based on literature with the corresponding references of the two of the five parameters selected for the shiny app.

Table 1. Feature Age extracted from "La Tabla" with its corresponding references.

WHO Tumor Type	Age	Citation
Anaplastic Astrocytoma, WHO grade III, IDH-mutated	57.25838	[74]
Anaplastic Astrocytoma, WHO grade III, IDH-wild type	56.17389	[74]
Anaplastic Ependymoma, Posterior Fossa A, WHO grade III	3.470269	[74]
Anaplastic Ependymoma, Posterior Fossa B, WHO grade III	30.15434	[74]
Anaplastic Ependymoma, Spine, WHO grade III	42.3617	[74]
Anaplastic Ependymoma, Supratentorial-RELA, WHO grade III	8.871502	[74]
Anaplastic Ependymoma, Supratentorial-YAP, WHO grade III	4.023892	[74]
Anaplastic Ganglioglioma	32.9504	[74]
Anaplastic Oligodendroglioma	52.94719	[74]
Anaplastic Pleomorphic Xanthoastrocytoma	25.40757	[22], [44]
Angiocentric Glioma	20.1175	[57]
Astroblastoma	20.91529	[75]
Astrocytoma, WHO grade II, IDH-Mutated	37.82914	[74]
Astrocytoma, WHO grade II, IDH-wild type	38.05708	[74]
Atypical Choroid Plexus Papilloma, WHO grade II	37.63072	[75]
Atypical Rhabdoid Tumour	8.161617	[38], [74]
Central Neurocytoma	29.80568	[38], [75]
Cerebellar Liponeurocytoma, WHO grade II	49.97034	[75]
Choroid Glioma Of The Third Ventricle	36.30717	[38], [75]
Choroid Plexus Carcinoma	24.94233	[38]
Choroid Plexus Papilloma	27.08243	[38]
Desmoplastic Infantile Astrocytoma, WHO grade I	1.605161	[125]
Desmoplastic Infantile Ganglioglioma	4.188498	[125]
Diffuse Leptomeningeal Glioneuronal Tumour	12.22865	[75]
Diffuse Midline Glioma, WHO grade IV	14.7292	[75]
Diffuse Oligodendroglioma, WHO grade II	46.10527	[75]
Dysembryoplastic Neuroepithelial Tumor	10.91598	[75]

Dysplastic Cerebellar Gangliocytoma, WHO grade I	38.08859	[75]
Ependymoma, Posterior Fossa A, WHO grade II	4.589818	[75]
Ependymoma, Posterior Fossa B, WHO grade II	30.41535	[75]
Ependymoma, Spine, WHO grade II	42.31803	[75]
Ependymoma, Supratentorial-YAP, WHO grade II	4.119103	[75]
Ependymoma, Supratentorial, RELA, WHO grade II	8.636612	[75]
Extraventricular Neurocytoma	40.17644	[75]
Gangliocytoma, WHO grade I	31.83199	[38]
Ganglioglioma	22.12451	[75]
Glioblastoma, IDH-mutated	50.51262	[75]
Glioblastoma, IDH-wild type	60.90557	[75]
Medulloblastoma, non-WNT/non-SHH, WHO grade IV	25.58433	[75]
Medulloblastoma, SHH Class, WHO grade IV	15.56225	[75]
Medulloblastoma, WNT Group, WHO grade IV	13.41433	[75]
Meningioma,WHO grade I	60.61425	[75]
Myxopapillary Ependymoma	36.30467	[27]
Paraganglioma	38.12739	[75]
Pilocytic Astrocytoma	22.16353	[38], [74]
Pilomyxoid Astrocytoma	1.614674	[38], [83]
Pleomorphic Xanthoastrocytoma, WHO grade II	29.37606	[38], [100]
Rosette-forming Glioneuronal Tumors, WHO grade I	27.18834	[129]
Schwannoma, WHO grade I	58.32085	[75]
Solitary Fibrous Tumour/Hemangiopericytoma Grade I	43.00789	[75]
Subependymal Giant Cell Astrocytoma, WHO grade I	14.20517	[92]
Subependymoma	37.37762	[38], [61]

Table 2. Feature Ki-67 extracted from "La Tabla" with its corresponding references.

WHO Tumor Type	**Ki-67**	**Citation**
Anaplastic Astrocytoma, WHO grade III, IDH-mutated	26.40252	[123]
Anaplastic Astrocytoma, WHO grade III, IDH-wild type	26.33504	[123]
Anaplastic Ependymoma, Posterior Fossa A, WHO grade III	12.69119	[75]
Anaplastic Ependymoma, Posterior Fossa B, WHO grade III	12.69119	[75]
Anaplastic Ependymoma, Spine, WHO grade III	12.68655	[75]
Anaplastic Ependymoma, Supratentorial-RELA, WHO grade III	12.84834	[75]
Anaplastic Ependymoma, Supratentorial-YAP, WHO grade III	12.96476	[75]
Anaplastic Ganglioglioma	32.70641	[75]
Anaplastic Oligodendroglioma	21.65347	[75]
Anaplastic Pleomorphic Xanthoastrocytoma	12.74161	[75]
Angiocentric Glioma	2.022847	[101], [105]

Astroblastoma	2.991548	[101]
Astrocytoma, WHO grade II, IDH-Mutated	5.494821	[123]
Astrocytoma, WHO grade II, IDH-wild type	5.429927	[123]
Atypical Choroid Plexus Papilloma, WHO grade II	13.01322	[31]
Atypical Rhabdoid Tumour	57.92757	[75]
Central Neurocytoma	1.996661	[75]
Cerebellar Liponeurocytoma, WHO grade II	3.792935	[75]
Choroid Glioma Of The Third Ventricle	0.0199971	[101]
Choroid Plexus Carcinoma	49.33664	[31]
Choroid Plexus Papilloma	1.900278	[31]
Desmoplastic Infantile Astrocytoma, WHO grade I	1.999507	[101]
Desmoplastic Infantile Ganglioglioma	3.064397	[101]
Diffuse Leptomeningeal Glioneuronal Tumour	0.5009569	[99]
Diffuse Midline Glioma, WHO grade IV	15.76368	[11] ,[120]
Diffuse Oligodendroglioma, WHO grade II	5.172283	[11]
Dysembryoplastic Neuroepithelial Tumor	1.962428	[101]
Dysplastic Cerebellar Gangliocytoma, WHO grade I	5.052819	[75]
Ependymoma, Posterior Fossa A, WHO grade II	1.084873	[75]
Ependymoma, Posterior Fossa B, WHO grade II	1.115519	[75]
Ependymoma, Spine, WHO grade II	1.113177	[75]
Ependymoma, Supratentorial-YAP, WHO grade II	1.139871	[75]
Ependymoma, Supratentorial, RELA, WHO grade II	1.107576	[75]
Extraventricular Neurocytoma	8.069866	[91]
Gangliocytoma, WHO grade I	2.001002	[75]
Ganglioglioma	1.793866	[75]
Glioblastoma, IDH-mutated	38.69587	[122]
Glioblastoma, IDH-wild type	39.00361	[75]
Medulloblastoma, non-WNT/non-SHH, WHO grade IV	36.01142	[75]
Medulloblastoma, SHH Class, WHO grade IV	28.6244	[75]
Medulloblastoma, WNT Group, WHO grade IV	19.73859	[75]
Meningioma,WHO grade I	5.600289	[75]
Myxopapillary Ependymoma	0.9929882	[77]
Paraganglioma	2.714961	[75]
Pilocytic Astrocytoma	5.226825	[101]
Pilomyxoid Astrocytoma	5.203091	[75], [120]
Pleomorphic Xanthoastrocytoma, WHO grade II	6.022234	[81]
Rosette-forming Glioneuronal Tumors, WHO grade I	4.18537	[129]
Schwannoma, WHO grade I	2.488276	[75]

Solitary Fibrous Tumour/Hemangiopericytoma Grade I	4.684723	[75]
Subependymal Giant Cell Astrocytoma, WHO grade I	2.875666	[117]
Subependymoma	6.117688	[33], [67]

One major limitation of “La Tabla” was the lack of probabilities in the given data within some articles. As a result, it was decided to transform the words “always”, “frequently”, “usually”, “often”, “sometimes”, “occasionally”, “seldom”, “rarely” and “never or N/A” in to probabilities: 100%, 90%, 80%, 70%, 50%, 40%, 20%, 10% and 0%, respectively.

The second limitation that was noticed during the completion of “La Tabla” was the controversial data found within different sources. For example, in Table 2., the mean age of the Atypical Rhabdoid Tumour was found to be 2 years following the 2007 WHO Classification of Tumors of the Central Nervous System, and 23 years following the CBTRUS data base. This problem was solved by calculating the weighted average between both sources. In this case, the result was equal to 8.161617.

2. R code.

Once “La Tabla” was completed, each tumor type was coded with a program called R studio, which is an open source software program mostly used for statistical analysis and developed by S language (Tutorialspoint, 2020).

This interface was used in order to create a database with individual files of each tumor type, that include the information collected from the Excel table. For that, different functions were created depending on the type of information and were added into a data frame. A data frame is a two-dimensional array structure in which each column contains values of one variable and each row contains one set of values from each column. The data can be either numerical or a character type (Tutorialspoint, 2020). An example of a numeric variable could be

age, for example the mean age for glioblastoma is 61.3 (WHO, 2016). General site is an example of a categorical variable since brainstem and frontal lobe do not account for numbers. In order to link the number of probabilities of developing each tumor in a certain brain region, a function was created.

```
site_function <- function(x, probability)  {

  site <- c("Frontal", "Temporal", "Parietal", "Occipital", "Deeper Structures of cerebrum","Ventricles", "Cerebellum", "Brainstem")

  prob_site <- sample(site, size = nrow(x), replace = TRUE, prob = probability)
  x$site <- prob_site
  return(x)
}
glioblastoma_adult_cohort <- site_function(glioblastoma_adult_cohort, probability = c(0.4, 0.29, 0.14, 0.03, 0.064, 0.022, 0.015, 0.041))
```

Figure 3. Function created with Rstudio in order to match the probabilities within each region of the brain where this type of glioblastoma can be found. For example, forty percent of the glioblastomas have the frontal lobe involved.

For the gender ratio, it was decided to arrange the value 1 to females and the value 0 to males. The rest of variables like low cellularity, infiltrative diffuse and EGFR amplification were coded in the same way. Similar functions to figure 3 were created in which the percentage originally found in “La Tabla” was placed to set certain probabilities.

```
mgmt_function <- function(x, probability, mgmt)  {

  result <- c(0,1)
  prob_result <- sample(result, size = nrow(x), replace = TRUE, prob = probability)
  x$test <- prob_result
  names(x)[ncol(x)] = mgmt
  return(x)
}
glioblastoma_adult_cohort <- mgmt_function(glioblastoma_adult_cohort, probability = c(.55,.45), mgmt = "MGMT")
```

Figure 4. The probability of finding MGMT in glioblastomas is of 45%, therefore, there are 55% of probability that MGMT will not be found within glioblastomas.

Ki67 was coded in a similar way than the variable age. Since both variables are numerical, the mean as well as the standard deviation were included.

```
ki67_function <- function(x, my_mean, my_sd)   {

  my_length <- nrow(x)
  my_ki67 <- abs(rnorm(my_mean, n = my_length, sd = my_sd))
  x$ki67 <- my_ki67
  return(x)

}


glioblastoma_adult_cohort <- ki67_function(glioblastoma_adult_cohort, my_mean  = 38.7, my_sd = 7.19)
```

Figure 5. Function created for the numerical variable ki67 that included the mean and the standard deviation found from literature. In this case the mean accounts for my_mean and it is equal to 38.7 and the standard deviation accounts for my_sd and it is equal to 7.19.

Each diagnosis was integrated in to the data frame with the diagnosis_function.

The following figure represents an example of the function created for diagnosis:

```
diagnosis_function <- function(x, my_diagnosis)  {

  x$diagnosis <- rep(my_diagnosis, times = nrow(x))

  return(x)
}
glioblastoma_new_df <- data.frame(glioblastoma_new_df, my_diagnosis = "Glioblastoma")
```

Figure 6. Diagnosis_function was created in order to add the type of diagnosis in to each tumor type data frame. This example is adding Glioblastoma as the final diagnosis in to the data frame.

Finally, each tumor type was individually saved in to the working directory in two formats: .R

and .csv. This was done using the saveRDS as well as the write.csv functions.

```
saveRDS(glioblastoma_new_df, file = "glioblastoma_adult_cohort.R")
write.csv(glioblastoma_new_df, file = "glioblastoma_adult_cohort.csv")
```

Figure 7. This is an example of how the glioblastoma data frame was saved within the computer using the saveRDS and write.csv functions.

Some diagnosis, including glioblastomas, share direct and indirect relationships with IHC and molecular data. These correlations had to be coded in a different way. Figure 8, shows an example of how IDH mutation is related with ATRX loss. In this example, if glioblastoma accounts for positive IDH mutation, there will be an 85% of probabilities that ATRX loss will be positive as well. The same coding process was repeated with EGFR amplification.

Finally, all the coded gliomas were merged in to a csv. data table that will be used in the next steps

```
glioblastoma_idh_pos <- subset(glioblastoma_new_df, idh1.R132H  == 1)
glioblastoma_idh_neg <- subset(glioblastoma_new_df, idh1.R132H  != 1)
nrow(glioblastoma_adult_cohort)
nrow(glioblastoma_idh_pos)
nrow(glioblastoma_idh_neg)
nrow(glioblastoma_idh_pos)/nrow(glioblastoma_adult_cohort)
test <- c(0, 1)
glioblastoma_idh_pos$ATRX.loss <-   sample(test, nrow(glioblastoma_idh_pos), replace = TRUE, prob = c(.15, .85)  )
glioblastoma_idh_pos$idh1.idh2 <- rep(1, times = nrow(glioblastoma_idh_pos))
glioblastoma_idh_neg$idh1.idh2 <- sample(test, nrow(glioblastoma_idh_neg), replace = TRUE, prob = c(.8, .2)  )
```

Figure 8. Relationship between IDH mutation and ATRX loss in glioblastoma.

3. Model Generated

XGBoost is a machine learning algorithm that implements decision trees designed for speed and performance on tabular datasets on classification and regression predictive modeling problems (Brownlee, 2019). It is a software library that can be downloaded and installed on R studio and implements the gradient boosting decision tree algorithm (which produces predicting models). It is used in a wide range of computing environments like parallelization of tree construction, distributed computing in order to train long models using clustered machines and caching optimization (Brownlee,2019).

C5.0 algorithm performs decision trees using entropy (indicates how incorporated the class values are) for measuring purity. The number zero, 0, will indicated that the sample is homogeneous or completely mixed. The number one, 1, applies when the sample is completely separated or heterogeneous (Yobero, 2018).

The algorithm random forest gives an approach in which each observation is fitted into every decision tree created. The most common outcome for each observation is used as the final input. Also, a new observation is included into each tree and it takes the greater number of votes for each classification model (R, 2020).

In order to select the most relevant features within the brain tumor data set, the Boruta algorithm was applied. This algorithm duplicates and shuffles the values in each column. To ensure the accuracy of these features, Boruta trained the random forest classifier in order to validate the importance of the feature by comparing it with random shuffled copies (Pathack, 2018). After this process, the Boruta algorithm selected the most relevant features: mostly clinical parameters (age, ki67, gender, tumor location) and data on histological architecture (endothelial proliferation, cellularity type and etc.). However, it was decided to only include clinical data and ki67 to the shiny app to formulate a test example. The accuracy of the RF model on data from “La Tabla” managed to reach ~ 60% in the absence of IHC, histology and molecular data. However, in order to increase the accuracy of the model on data obtained from patients at OSU we had to add additional features on distinct histological architecture to the model. Using 19 features in total our model managed to predict the diagnosis of 100 OSU patients with 84% accuracy and “La Tabla” data (94%) in the absence of molecular and IHC features (p53, ATRX, IDH status and etc.)

	x
Accuracy	0.8437500
Kappa	0.7834261
AccuracyLower	0.7554159
AccuracyUpper	0.9098275
AccuracyNull	0.4687500
AccuracyPValue	0.0000000
McnemarPValue	NaN

Figure 9. Random Forest model showing 84% of accuracy using 19 features over 100 OSU patients.

```
Overall Statistics

               Accuracy : 0.9494
                 95% CI : (0.947, 0.9518)
    No Information Rate : 0.0557
    P-Value [Acc > NIR] : < 2.2e-16

                  Kappa : 0.9482

 Mcnemar's Test P-Value : NA
```

Figure 10. Random Forest shows a 94% accuracy when predicting diagnosis with data extracted from "La Tabla".

Although XGBoost and C5.0 algorithms proved to be less accurate using same features as the Random Forest algorithm, they could still predict the diagnosis on real patient dataset with moderate accuracy - 78% and 72% respectively in the absence of IHC and molecular data.

4. Shiny app.

Shiny App is a package within R studio that provides the opportunity of creating interactive web applications. In order to create a functional Shiny App, it is important to understand how it

is organized. Each Shiny App has two parts: UI, or user interface, and the server. The UI is HTML that you use while constructing Shiny functions, it shows the user how the layout of the web is arranged. The server part is used to make the app interactive for the user. All Shiny Apps have the same template. In order to build Shiny Apps, a template is created that will be composed of the package "shiny" as well as an empty UI and server

```
library(shiny)
ui <- fluidPage()
server <- function(input, output) {}
shinyApp(ui = ui, server = server)
```

Figure 11. Template for a Shiny App

For our Shiny App, the package "randomForest" was downloaded since in order to make predictions, the model Random Forest is required to be fitted in to the app. The R file with all the gliomas coded as well as the Random Forest model file were imported to the Shiny App using the function readRDS. Since the variables general and specific site are categorical, they were switched to factor so they could be incuded in to the data frame.

```
library(shiny)
library(randomForest)

glioma <- readRDS("/Users/yolandacabello/Desktop/May_project/testRstudio/testwithbarplot/glioma_fixed.R")
rf_model <- readRDS("/Users/yolandacabello/Desktop/May_project/testRstudio/testwithbarplot/Yolanda_Shiny_clin_ki67_rf).R")
glioma$Specific.site <- as.factor(glioma$Specific.site)
glioma$General.site <- as.factor(glioma$General.site)
```

Figure 12. Code used for Glioma Modelling App for importing models and downloaded packages.

The inputs are functions placed by the user in order to create values or interactions. They are coded within the fluidpage () function. In this case, it was decided to include gender,

age, ki67, general and specific site with different types of inputs. For that, this is the code that it was used:

```
ui <- fluidPage(

  titlePanel("Glioma Modeling Project"),
  sidebarPanel(

    sliderInput(inputId = 'age',
                label = "Please select your age",
                min = 1,
                max = 100,
                value = 30),
    sliderInput(inputId = 'ki67',
                label = "Please select your ki67",
                min = 1,
                max = 100,
                value = 30),
    radioButtons("gender", "Please select your gender:",
                 c("Male" = 0,
                   "Female" = 1)),
    selectInput("ssite",
                label = "Choose Specific Anatomical Site:",
                choices = c(levels(glioma$Specific.site))),

    selectInput("gsite",
                label = "Choose General Anatomical Site:",
                choices = c(levels(glioma$General.site))),

    submitButton("Apply Changes")
      ),
```

Figure 13. Glioma Modelling App code for the UI interface.

In Figure 13, it is noticeable that there were used three different types of inputs: sliderInput, radioButtons, selectInput and a submitButton that will update the information placed on the inputs when clicked. It was decided to use different inputs because the information that these inputs carry are different. For example, age represents a number while general site represents multiple places within the brain. Therefore, we considered it appropriate to do it this manner.

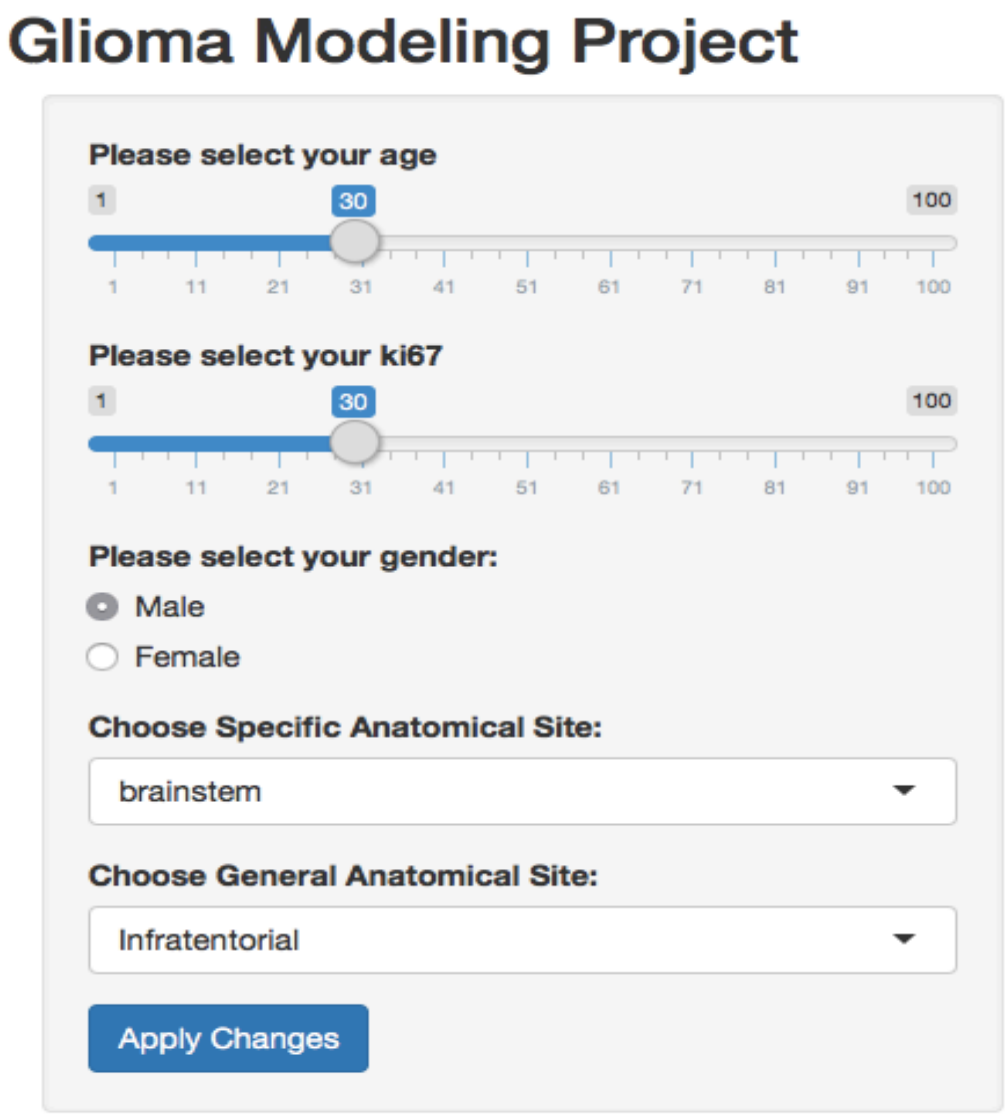

Figure 14. Different inputs for the Glioma Modelling App.

The server part requires to fit the model within the function. For that, a data frame was created in order to link the inputs with the variables coded within the glioma file. An example that can be observed in Figure 5, it is that "General.site" is how this variable was named in the glioma file and it is equal to "input$gsite" which is making reactive the id input gsite (which it is observed in Figure 3). Therefore, once we choose a general anatomical sites in the input, this

will pick the information from the glioma file and will react with the inputs to show the selected information.

After the data frame was created, the prediction of the randomForest model was set up giving place to a bar plot that will only include the top five diagnosis with the highest probabilities. For that, the barplot() as well as the predict() functions were used.

```
server <- function(input, output) {

  output$distPlot <- renderPlot({
    df <- data.frame("Age" =  as.numeric(input$age),
                     "Gender" = as.numeric(input$gender), "ki67" = input$ki67,
                     "General.site" = input$gsite, "Specific.site" = input$ssite)
   levels(df$General.site) = levels(glioma$General.site)
   levels(df$Specific.site) = levels(glioma$Specific.site)

    data <- predict(rf_model, df, type = "prob")

    d1 <- t(data)
    d1 <- data.frame("Probability" = d1[,1], "Diagnosis" = rownames(d1))
    d1
    a <- order(d1$Probability, decreasing = TRUE)
    d1 <- d1[a,]
    d2 <- d1[1:5,]
    colors <- c("Red", "Light Blue", "Orange", "Yellow", "Pink")
    barplot(d2$Probability, names.arg = d2$Diagnosis, las =1, ylim = c(0, 1),cex.axis = 0.7, cex.names = 0.50, font = 2, col = colors)
    legend("topright", fill = colors, legend = d2$Diagnosis)


  })

}

# Run the application
shinyApp(ui = ui, server = server)
```

Figure 15. Server function for the Glioma Modelling App.

The only output implicit within the server function is called “distPlot” and it is linked to a bar plot. For making a Shiny App reactive, it is necessary to include the name of the output (in this case is distPlot() within the main panel.

```
        mainPanel(
          plotOutput("distPlot"),
        )
)
```

Figure 16. Creating reactivity in the Glioma Modelling App.

Once both of the parts were filled (the UI and the server), the application was ran and this was the result:

Figure 17. Completed app for Glioma Modelling Project.

The theme that it is usually used for a regular Shinny App was switched in to the "superhero" shiny theme in order to give the web page a different look compared to regular Shiny Apps. A limitation was experienced during this method since the diagnosis under each bar plot are extremely small, it was decided to create a legend with the legend() function in order to clarify the possible diagnosis.

Results and Discussion

Glioma Modelling Project was originally created in order to simplify and avoid additive expenses of some laboratory processes that some hospitals do not have. In this way, third world countries would not have the means to amplify their laboratories; pathologists would just need a few of not expensive medical proves required to fill the parameters within the shiny app to obtain the probability of the five tumors with most possibilities of being diagnosed for a specific patient.

Since the most updated version of The World Health Organization has around 200 different types of tumors, it was decided to select the 53 most common tumor diagnoses from both adult and pediatric types. This decision was made because the lack of information in literature and academic articles about some tumor diagnosis. Therefore, the first limitation that was experienced during this project, was the absence of information about some very specific tumor types.

Along with this limitation, it was decided to dismiss some categories of “La Tabla” based on the Boruta algorithm, which was used in order to select the most relevant features for our study.These features account for clinical and histological architecture. Even though the Boruta algorithm selected more categories as ~~a~~ shadow features (features with higher Z-score), it was decided to only include clinical data which included gender, age, general and specific sites, as well as ki67 because it predicted diagnosis with an accuracy of 60% with the random forest algorithm.

Another major limitation of this study was the failed accuracy of diagnosing some types of brain tumors. This is because the random forest algorithm only has 60% of accuracy. An example of this would be when the pediatric tumor Pleomorphic Xanthoastrocytoma should be diagnosed when the parameters selected are: five for age, seven for ki67, and the locations are posterior fossa and infratentorial. However, the type of tumor that was diagnosed following these parameters was Diffuse Midline Glioma, WHO grade IV with more than a 70% ~~of~~ probability. This is a pediatric tumor as well and it usually has a low ki67, but it is not commonly found within the posterior fossa. Thus, this is an example in which the shiny app is not accurate enough.

Figure 18. Shiny app showing an inaccurate diagnosis.

There was a study made in September of 2016 named "An Automatic Classification of Brain Tumors through MRI Using Support Vector Machine" that distinguished between benign and malignant tumors with an accuracy of 98.9% using an algorithm called Support Vector

Machine. This algorithm was used in order to recognize large tumors in MRI's from the surrounding tissues of the brain while compared to normal brain images (Alfonse et al, 2016). The study results are relevant to the Glioma Modelling Project in order to contemplate different approaches to get the same results while using MRI images. Also, the algorithm SVM, which is classified as a supervised model, could be used as a tool in order to train our glioma data to observe features that the algorithm includes. It also observes which features it excludes and the accuracy percentage of the prediction.

There is another recent study called "MethPed: an R package for the identification of pediatric brain tumor subtypes" that uses the random forest algorithm in order to predict pediatric brain tumors. The prediction was done by using DNA methylation parameters. The R package predicts five groups of brain tumors: glioblastomas, medulloblastomas, diffuse intrinstic pontine gliomas, ependymomas and embryonal tumors with multilayered rosettes. Diagnosis that do not fit any of these categories will be determined as inconclusive (Ahamed et al, 2016). This study resulted very interesting since the same algorithm was performed, however, this study only predicted a small group of brain tumors excluding adult cases and did not give any information about the accuracy of the predictions that the package made. Therefore, the lack of official results makes this study not reliable even if the method that was used to create the predictions was the same in both studies.

For future directions, I would suggest to increase the accuracy of the prediction of tumor diagnosis in order to avoid the wrong diagnosis of some brain tumors. This could be solved by the addition of molecular as well as histochemical data in to the random forest model. After that, the addition of these new features in to the shiny app. If the random forest

does not increase its accuracy by adding molecular and histochemical data, other algorithms like support vector machine could be tested in our model. Also, the addition of more tumor types in to the shiny app could provide neuropathologists the certainty of not excluding some possible diagnosis.

Our team is currently using OSU real patient data to compare the real results with the predicted results given by the shiny app.

Once the accuracy it is increased enough that the website could be considered as credible and reliable, I believe that the promotion of the shiny app would be an excellent idea. This project could be promoted through social and professional media. Since the main goal of this project it always has been to extend the idea of using artificial intelligence to diagnose brain tumors in order to make possible this kind of diagnosis without using expensive laboratory techniques, I believe that a lot of hospitals around the world could potentially be interested on acquiring this tool. For that, I would suggest to offer this tool worldwide for free.

Further on, this project could also be used as a study tool for neuropathologist's and neuro-oncologist's students. Since all the predictions were done based on decision trees; the same method can be developed for future neurology students in order to provide them an idea of which data a tumor is more likely to have.

The findings of this study can be understood as the creation of a free webpage that in a future will be a worldwide open resource for doctors as well as for medical students that are interested on neuropathology. Also, the eradication of highly costly medical techniques saving the patients some money up. Therefore, more patients could afford the diagnosis and

treatment of brain tumors. Thus, once this tool is fully developed, the Glioma Modelling Project could help the world saving more human lives.

Glossary:

Sensitivity: measures how often a test correctly generates a positive result for people who have the condition that is being tested for. For example, a test that is highly sensitive will flag almost everyone who has the disease and not generate many false negative results (Health News Review).

Specificity: measures a test's ability to correctly generate a negative result for people who do not have the condition that is being tested for. One example is that a high specificity test will correctly rule out almost everyone who does not have the disease and will not generate many false positive results (Health News Review).

Accuracy: refers to the correctness of a single measurement. It is determined by comparing the measurement against the true or accepted value. An accurate measurement is close to the true value. For example, hitting the center of a bullseye (Helmenstine, 2018).

Positive Predictive Value (PPV): The likelihood that an individual with a positive test result truly has the particular gene and/or disease in question (NCI Dictionary of Cancer Terms).

References.

1. “Brain Tumors.” *AANS*, www.aans.org/en/Patients/Neurosurgical-Conditions-and-Treatments/Brain-Tumors.

2. “CBioPortal for Cancer Genomics.” *CBioPortal for Cancer Genomics*, www.cbioportal.org/.

3. “Central Nervous System, Embryonal Tumors.” Central Nervous System, Embryonal Tumors | University Hospitals, www.uhhospitals.org/rainbow/services/pediatric-cancer-and-blood-disorders/conditions-and-treatments/central-nervous-system-embryonal-tumors

4. “Choroid Plexus Carcinoma.” Choroid Plexus Carcinoma - an Overview | ScienceDirect Topics, www.sciencedirect.com/topics/medicine-and-dentistry/choroid-plexus-carcinoma.

5. “Choroid Plexus Papilloma.” Background, Problem, Epidemiology, 17 Apr. 2019, emedicine.medscape.com/article/250795-overview.

6.“Confusion Matrix in Machine Learning.” *GeeksforGeeks*, 7 Feb. 2018, www.geeksforgeeks.org/confusion-matrix-machine-learning/.

7.“Data Frames.” *R*, Tutorialspoint, 2020, www.tutorialspoint.com/r/r_data_frames.htm.

8. “Definition of PPV - NCI Dictionary of Cancer Terms.” *National Cancer Institute*, www.cancer.gov/publications/dictionaries/genetics-dictionary/def/ppv.

9. “Final Diagnosis -- Mixopapillary Ependymoma, WHO Grade 1.” Final Diagnosis -- Case 626, path.upmc.edu/cases/case626/dx.html.

10. “Glioblastoma and Malignant Astrocytoma.” *AMERICAN BRAIN TUMOR ASSOCIATION*, Www.abta.org 3, www.abta.org/wp-content/uploads/2018/03/glioblastoma-brochure.pdf.

11. “INTERNATIONAL AGENCY FOR RESEARCH ON CANCER.” *IARC*, www.iarc.fr/.

12. “Lhermitte-Duclos Disease (Dysplastic Gangliocytoma of the Cerebellum).” Clinical Neurology and Neurosurgery, Elsevier, 13 June 2001, www.sciencedirect.com/science/article/pii/S030384670100124X?via=ihub.

13. “Massachusetts General Hospital.” Massachusetts General Hospital, Boston, MA, www.massgeneral.org/tsc/patient-ed/brain-anatomy.aspx.

14. “Primitive Neuro-Ectodermal Tumors (PNET).” National Cancer Institute, www.cancer.gov/nci/rare-brain-spine-tumor/tumors/pnet.

15. “Random Forest.” *R*, 2020, www.tutorialspoint.com/r/r_random_forest.htm.

16.“Understanding Medical Tests: Sensitivity, Specificity, and Positive Predictive Value.” *HealthNewsReview.org*, www.healthnewsreview.org/toolkit/tips-for-understanding-studies/understanding-medical-tests-sensitivity-specificity-and-positive-predictive-value/.

17.“What Is Machine Learning? A Definition.” *Expert System*, 11 Nov. 2019, expertsystem.com/machine-learning-definition/.

18. Adesina, A. M., & Rauch, R. A. (2010). Dysembryoplastic neuroepithelial tumor. Atlas of Pediatric Brain Tumors, 171–180. https://doi.org/10.1007/978-1-4419-1062-2_17.

19. Ahamed, Mohammad Tanvir, et al. “MethPed: an R Package for the Identification of Pediatric Brain Tumor Subtypes.” *BMC Bioinformatics*, BioMed Central, 2 July 2016, www.ncbi.nlm.nih.gov/pmc/articles/PMC4930602/.

21. Aibaidula, Abudumijit, et al. “Adult IDH Wild-Type Lower-Grade Gliomas Should Be Further Stratified.” Neuro-Oncology, Oxford University Press, Oct. 2017, www.ncbi.nlm.nih.gov/pmc/articles/PMC5596181/.

22. Alexandrescu, Sanda, et al. “Epithelioid Glioblastomas and Anaplastic Epithelioid Pleomorphic Xanthoastrocytomas-Same Entity or First Cousins?” Brain Pathology, John Wiley & Sons, Ltd (10.1111), 22 Sept. 2015, onlinelibrary.wiley.com/doi/epdf/10.1111/bpa.12295.

23. Alfonse, Marco, and Abdel-Badeeh M. Salem. “An Automatic Classification of Brain Tumors through MRI Using Support Vector Machine.” *Egyptian Computer Science Journal*, Egyptian Computer Science Journal, Sept. 2016, ecsjournal.org/Archive/Volume40/Issue3/2.pdf.

24. Amatya, V. J., Akazawa, R., Sumimoto, Y., Takeshima, Y., & Inai, K. (2009). Clinicopathological and immunohistochemical features of three pilomyxoid astrocytomas: Comparative study with 11 pilocytic astrocytomas. Pathology International, 59(2), 80–85. https://doi.org/10.1111/j.1440-1827.2008.02332.x.

25. Ampie, Leonel, et al. “Clinical Attributes and Surgical Outcomes of Angiocentric Gliomas.” Journal of Clinical Neuroscience, Churchill Livingstone, 8 Jan. 2016, www.sciencedirect.com/science/article/pii/S0967586815006542.

26. Arora, Ramandeep S, et al. “Age-Incidence Patterns of Primary CNS Tumors in Children, Adolescents, and Adults in England.” Neuro-Oncology, Duke University Press, Aug. 2009, www.ncbi.nlm.nih.gov/pmc/articles/PMC2743220/.

27. Barton, Valerie N, et al. “Unique Molecular Characteristics of Pediatric Myxopapillary Ependymoma.” Brain Pathology (Zurich, Switzerland), Blackwell Publishing Ltd, May 2010, www.ncbi.nlm.nih.gov/pmc/articles/PMC2871180/.

28. Bianchi, F., Tamburrini, G., Gessi, M. et al. Childs Nerv Syst (2018) 34: 817. https://doi.org/10.1007/s00381-018-3764-3.

29. Blakeley, Jaishri, and Stuart Grossman. “Anaplastic Oligodendroglioma.” July 2008, www.ncbi.nlm.nih.gov/pmc/articles/PMC3994534/?report=reader.

30. BLUMCKE, INGMAR. SARNAT, HARVEY B. CORAS, ROLAND. *SURGICAL NEUROPATHOLOGY OF FOCAL EPILEPSIES: Textbook & Atlas*. JOHN LIBBEY EUROTEXT, 2015.

31. BOHARA, M., HIRABARU, M., FUJIO, S., HIGASHI, M., YONEZAWA, H., KARKI, P., … ARITA, K. (2015). Choroid Plexus Tumors: Experience of 10 Cases with Special References to Adult Cases. Neurologia Medico-Chirurgica, 55(12), 891–900. https://doi.org/10.2176/nmc.oa.2015-0126

32. Brownlee, Jason. “A Gentle Introduction to XGBoost for Applied Machine Learning.” *Machine Learning Mastery*, 21 Aug. 2019, machinelearningmastery.com/gentle-introduction-xgboost-applied-machine-learning/.

33. Bruger, Peter, and Bernd Scheithauer. *Diagnostic Pathology: Neuropathology*. Amirsys, 2012.

34. Buccoliero, A. M., Franchi, A., Castiglione, F., Gheri, C. F., Mussa, F., Giordano, F., … Taddei, G. L. (2009). Subependymal giant cell astrocytoma (SEGA): Is it an astrocytoma? Morphological, immunohistochemical and ultrastructural study. Neuropathology, 29(1), 25–30. https://doi.org/10.1111/j.1440-1789.2008.00934.x.

35. Bugiani, M., van Zanten, S. E. M. V., Caretti, V., Schellen, P., Aronica, E., Noske, D. P., … Hulleman, E. (2017). Deceptive morphologic and epigenetic heterogeneity in diffuse intrinsic pontine glioma. Oncotarget, 8(36), 60447–60452. https://doi.org/10.18632/oncotarget.19726.

36. Burger, Peter C., et al. *Surgical Pathology of the Nervous System and Its Coverings*. Churchill Livingstone, 2002.

37. Carangelo, B. (2015). Papillary glioneuronal tumor: case report and review of literature. Giornale Di Chirurgia - Journal of Surgery, 36(April), 63–69. https://doi.org/10.11138/gchir/2015.36.2.063.

38. CBTRUS. Statistical Report: Primary Brain Tumors in the United States, 1997–2001. Central Brain Tumor Registry of the United States. 2004.

39. Cerdá-Nicolás, M., Lopez-Gines, C., Gil-Benso, R., Donat, J., Fernandez-Delgado, R., Pellin, A., … Barbera, J. (2006). Desmoplastic infantile ganglioglioma. Morphological, immunohistochemical and genetic features [8]. Histopathology, 48(5), 617–621. https://doi.org/10.1111/j.1365-2559.2005.02275.x.

40. Chatterjee, D., Radotra, B. D., Kumar, N., Vasishta, R. K., & Gupta, S. K. (2018). IDH1, ATRX, and BRAFV600E mutation in astrocytic tumors and their significance in patient outcome in north Indian population. Surgical Neurology International, 9, 29. https://doi.org/10.4103/SNI.SNI_284_17.

41. Cho, Hwa Jin, et al. “Primary Diffuse Leptomeningeal Glioneuronal Tumors.” SpringerLink, Springer Japan, 26 Apr. 2014, link.springer.com/article/10.1007/s10014-014-0187-z.

42. Collins, V. P., Jones, D. T. W., & Giannini, C. (2015). Pilocytic astrocytoma: pathology, molecular mechanisms and markers. Acta Neuropathologica, 129(6), 775–788. https://doi.org/10.1007/s00401-015-1410-7.

43. Crespo-Rodríguez, Ana M., et al. “MR and CT Imaging of 24 Pleomorphic Xanthoastrocytomas (PXA) and a Review of the Literature.” SpringerLink, Springer-Verlag, 5 Jan. 2007, link.springer.com/article/10.1007/s00234-006-0191-z.

44. Dudley, Roy W R, et al. “Pediatric Low-Grade Ganglioglioma: Epidemiology, Treatments, and Outcome Analysis on 348 Children from the Surveillance, Epidemiology, and End Results Database.” Neurosurgery, U.S. National Library of Medicine, Mar. 2015, www.ncbi.nlm.nih.gov/pmc/articles/PMC4333003/.

45. Ebrahimi, A., Skardelly, M., Bonzheim, I., Ott, I., Mühleisen, H., & Eckert, F. (2016). ATRX immunostaining predicts IDH and H3F3A status in gliomas. Acta Neuropathologica Communications, 1–10. https://doi.org/10.1186/s40478-016-0331-6.

46. Edgar, M. A., & Rosenblum, M. K. (2008). The differential diagnosis of central nervous system tumors: A critical examination of some recent immunohistochemical applications. Archives of Pathology and Laboratory Medicine, 132(3), 500–509.

47. Ellebogen, Richard, and Michael Scott. “Choroid Plexus Tumor.” Choroid Plexus Tumor - an Overview | ScienceDirect Topics, 2012, www.sciencedirect.com/topics/medicine-and-dentistry/choroid-plexus-tumor.

48. Engelhard, H. H., Stelea, A., & Cochran, E. J. (2002). Oligodendroglioma: Pathology and molecular biology. Surgical Neurology, 58(2), 111–117. https://doi.org/10.1016/S0090-3019(02)00751-6.

49. Fèvre-Montange, M., Szathmari, A., Champier, J., Mokhtari, K., Chrétien, F., Coulon, A., … Jouvet, A. (2008). Pineocytoma and pineal parenchymal tumors of intermediate differentiation presenting cytologic pleomorphism: A multicenter study. Brain Pathology, 18(3), 354–359. https://doi.org/10.1111/j.1750-3639.2008.00128.x.

50. Furuta, T., Miyoshi, H., Komaki, S., Arakawa, F., Morioka, M., Ohshima, K., … Sugita, Y. (2018). Clinicopathological and genetic association between epithelioid glioblastoma and pleomorphic xanthoastrocytoma. Neuropathology, 38(3), 218–227. https://doi.org/10.1111/neup.12459.

51. Gaillard, Frank. “Central Neurocytoma | Radiology Reference Article.” Radiopaedia Blog RSS, radiopaedia.org/articles/central-neurocytoma.

52. Giorgianni, Andrea, et al. “Lhermitte-Duclos Disease. A Case Report.” The Neuroradiology Journal, Centauro S.r.l., Dec. 2013, www.ncbi.nlm.nih.gov/pmc/articles/PMC4202883/#R6.

53. Gokden, M. (2017). If it is Not a Glioblastoma, Then What is it? A Differential Diagnostic Review. Advances in Anatomic Pathology, 24(6), 379–391. https://doi.org/10.1097/PAP.0000000000000170.

54. Graham, D., Magee, H., Kierce, B., Ball, R., Dervan, P., & O’Meara, A. (1995). Evaluation of Ki-67 Reactivity in Neuroblastoma Using Paraffin Embedded Tissue. Pathology Research and Practice, 191(2), 87–91. https://doi.org/10.1016/S0344-0338(11)80557-1.

55. Haberler, C., Laggner, U., Slavc, I., Czech, T., Ambros, I. M., Ambros, P. F., … Hainfellner, J. A. (2006). Immunohistochemical analysis of INI1 protein in malignant pediatric CNS tumors: Lack of INI1 in atypical teratoid/rhabdoid tumors and in a fraction of primitive

neuroectodermal tumors without rhabdoid phenotype. American Journal of Surgical Pathology, 30(11), 1462–1468. https://doi.org/10.1097/01.pas.0000213329.71745.ef.

56. Hashemi, F., Naderian, M., Kadivar, M., Nilipour, Y., & Gheytanchi, E. (2014). Expression of neuronal markers, NFP and GFAP, in malignant astrocytoma. Asian Pacific Journal of Cancer Prevention, 15(15), 6315–6319.

57. Hasselblatt, M., Blümcke, I., Jeibmann, A., Rickert, C. H., Jouvet, A., Van De Nes, J. A. P., … Paulus, W. (2006). Immunohistochemical profile and chromosomal imbalances in papillary tumours of the pineal region. Neuropathology and Applied Neurobiology, 32(3), 278–283. https://doi.org/10.1111/j.1365-2990.2006.00723.x.

58. He, Wen-Guang, et al. "Clinical and Biological Features of Neuroblastic Tumors: A Comparison of Neuroblastoma and Ganglioneuroblastoma." Oncotarget, Impact Journals LLC, www.ncbi.nlm.nih.gov/pmc/articles/PMC5514944/#!po=76.3158.

59. Helmenstine, Anne Marie. "What Is Accuracy in Science?" *ThoughtCo*, ThoughtCo, 2 Sept. 2018, www.thoughtco.com/definition-of-accuracy-in-science-604356.

60. Ishizawa, K., Komori, T., Shimada, S., & Hirose, T. (2011). Olig2 and CD99 are useful negative markers for the diagnosis of brain tumors. Clinical Neuropathology, 27(05), 118–128. https://doi.org/10.5414/npp27118.

61. Jain, Amit, et al. "Subependymoma: Clinical Features and Surgical Outcomes." Neurological Research, U.S. National Library of Medicine, 28 Sept. 2012, www.ncbi.nlm.nih.gov/pmc/articles/PMC4618470/.

62. Jouvet, A., Saint-Pierre, G., Fauchon, F., Privat, K., Bouffet, E., Ruchoux, M., … Fèvre-Montange, M. (2010). Pineal Parenchymal Tumors: A Correlation of Histological Features with

Prognosis in 66 Cases. Brain Pathology, 10(1), 49–60. https://doi.org/10.1111/j.1750-3639.2000.tb00242.x.

63. K. Ishizawa, T. Komori, S. Shimada and T. Hirose .Olig2 and CD99 are useful negative markers for the diagnosis of brain tumors . 2008; 27: 118-128. doi: 10.5414/NPP27118.

64. Kleinschmidt-Demasters, B. K., Aisner, D. L., Birks, D. K., & Foreman, N. K. (2013). Epithelioid GBMs show a high percentage of BRAF V600E mutation. American Journal of Surgical Pathology, 37(5), 685–698. https://doi.org/10.1097/PAS.0b013e31827f9c5e.

65. Koeller, Kelly, and Elizabeth Rushing. "Medulloblastoma: A Comprehensive Review with Radiologic-Pathologic Correlation1." RadioGraphics, From the Archives of the AFIP, pubs.rsna.org/doi/10.1148/rg.236035168?url_ver=Z39.882003&rfr_id=ori:rid:crossref.org&rfr_dat=cr_pub=pubmed&.

66. Kraetzig, Theresa, et al. "Metastases of Spinal Myxopapillary Ependymoma: Unique Characteristics and Clinical Management in: Journal of Neurosurgery: Spine Volume 28 Issue 2 (2018)." Journal of Neurosurgery: Spine, American Association of Neurological Surgeons, 24 Oct. 2018, thejns.org/spine/view/journals/j-neurosurg-spine/28/2/article-p201.xml.

67. Lamzabi, I., Arvanitis, L. D., Reddy, V. B., Bitterman, P., & Gattuso, P. (2013). Immunophenotype of myxopapillary ependymomas. Applied Immunohistochemistry and Molecular Morphology, 21(6), 485–489. https://doi.org/10.1097/PAI.0b013e318283980a.

68. Larjavaara, Suvi, et al. "Incidence of Gliomas by Anatomic Location." Neuro-Oncology, Duke University Press, July 2007, www.ncbi.nlm.nih.gov/pmc/articles/PMC1907421/.

69. Lee, Kyung-Hwa, et al. "Prognostic Significance of Neuronal Marker Expression in Glioblastomas." *Child's Nervous System : ChNS : Official Journal of the International Society for*

Pediatric Neurosurgery, U.S. National Library of Medicine, Nov. 2012, www.ncbi.nlm.nih.gov/pubmed/22922887.

70. Lee, S. J., Bui, T. T., Chen, C. H. J., Lagman, C., Chung, L. K., Sidhu, S., … Yang, I. (2016). Central Neurocytoma: A Review of Clinical Management and Histopathologic Features. Brain Tumor Research and Treatment, 4(2), 49. https://doi.org/10.14791/btrt.2016.4.2.49.

71. Li, Y., Ye, X. F., Qian, G., Yin, Y., & Pan, Q. G. (2012). Pathologic features and clinical outcome of central neurocytoma: Analysis of 15 cases. Chinese Journal of Cancer Research, 24(4), 284–290. https://doi.org/10.1007/s11670-012-0265-x.

72. Lin, G. G., & Scott, J. G. (2012). 一价铜生化的亲和力测定标准NIH Public Access, 100(2), 130–134. https://doi.org/10.1016/j.pestbp.2011.02.012.Investigations.

73. Linsenmann, T., Monoranu, C. M., Alkonyi, B., Westermaier, T., Hagemann, C., Kessler, A. F., … Löhr, M. (2019). Cerebellar liponeurocytoma - molecular signature of a rare entity and the importance of an accurate diagnosis. Interdisciplinary Neurosurgery: Advanced Techniques and Case Management, 16(October 2018), 7–11. https://doi.org/10.1016/j.inat.2018.10.017.

74. Louis, David N., et al. WHO Classification of Tumours of the Central Nervous System. International Agency for Research on Cancer, 2007.

75. Louis, David N., et al. WHO Classification of Tumours of the Central Nervous System. International Agency For Research On Cancer, 2016.

76. Luyken, C., Blümcke, I., Fimmers, R., Urbach, H., Wiestler, O. D., & Schramm, J. (2004). Supratentorial gangliogliomas: Histopathologic grading and tumor recurrence in 184

patients with a median follow-up of 8 years. Cancer, 101(1), 146–155. https://doi.org/10.1002/cncr.20332.

77. Lyle, M. R., Dolia, J. N., Fratkin, J., Nichols, T. A., & Herrington, B. L. (2015). Newly Identified Characteristics and Suggestions for Diagnosis and Treatment of Diffuse Leptomeningeal Glioneuronal/Neuroepithelial Tumors. Child Neurology Open, 2(1), 2329048X1456753. https://doi.org/10.1177/2329048x14567531.

78. Makuria, Addisalem T, et al. "Atypical Teratoid Rhabdoid Tumor (AT/RT) in Adults: Review of Four Cases." *Journal of Neuro-Oncology*, U.S. National Library of Medicine, July 2008, www.ncbi.nlm.nih.gov/pubmed/18369529.

79. Martinez-Diaz, H., Kleinschmidt-DeMasters, B. K., Powell, S. Z., & Yachnis, A. T. (2003). Giant cell glioblastoma and pleomorphic xanthoastrocytoma show different immunohistochemical profiles for neuronal antigens and p53 but share reactivity for class III β-tubulin. Archives of Pathology and Laboratory Medicine, 127(9), 1187–1191.

80. Martinez-Large, Maria, and John DeWitt. "Oligodendroglioma, IDH Mutant and 1p/19q Codeleted." *Pathology Outlines - PathologyOutlines.com*, June 2019, www.pathologyoutlines.com/topic/cnstumoroligodendrogliomaidhmutant.html.

81. Marton, E., Feletti, A., Orvieto, E., & Longatti, P. (2007). Malignant progression in pleomorphic xanthoastrocytoma: Personal experience and review of the literature. Journal of the Neurological Sciences, 252(2), 144–153. https://doi.org/10.1016/j.jns.2006.11.008; (2) WHO 2016, p96.

82. Matsumoto, T, et al. "MIB-1 and p53 Immunocytochemistry for Differentiating Pilocytic Astrocytomas and Astrocytomas from Anaplastic Astrocytomas and Glioblastomas in

Children and Young Adults." *Histopathology*, U.S. National Library of Medicine, Nov. 1998, www.ncbi.nlm.nih.gov/pubmed/9839169.

83. Matyja, Ewa, et al. "Heterogeneity of Histopathological Presentation of Pilocyticastrocytoma – Diagnostic Pitfalls. A Review." Folia Neuropathologica, vol. 3, 1 Jan. 2016, pp. 197–211., doi:10.5114/fn.2016.62530.

84. Mellai, M., Piazzi, A., Caldera, V., Monzeglio, O., Cassoni, P., Valente, G., & Schiffer, D. (2011). IDH1 and IDH2 mutations, immunohistochemistry and associations in a series of brain tumors. Journal of Neuro-Oncology, 105(2), 345–357. https://doi.org/10.1007/s11060-011-0596-3.

85. Mesturoux, L., Durand, K., Pommepuy, I., Robert, S., Caire, F., & Labrousse, F. (2016). Molecular analysis of tumor cell components in pilocytic astrocytomas, gangliogliomas, and oligodendrogliomas. Applied Immunohistochemistry and Molecular Morphology, 24(7), 496–500. https://doi.org/10.1097/PAI.0000000000000288.

86. Meurer, R. T., Martins, D. T., Hilbig, A., Ribeiro, M. de C., Roehe, A. V., Barbosa-Coutinho, L. M., & Fernandes, M. da C. (2008). Immunohistochemical expression of markers Ki-67, neun, synaptophysin, p53 and HER2 in medulloblastoma and its correlation with clinicopathological parameters. Arquivos de Neuro-Psiquiatria, 66(2b), 385–390. https://doi.org/10.1590/s0004-282x2008000300020.

87. Min, H. S., Lee, Y. J., Park, K., Cho, B. K., & Park, S. H. (2006). Medulloblastoma: Histopathologic and molecular markers of anaplasia and biologic behavior. Acta Neuropathologica, 112(1), 13–20. https://doi.org/10.1007/s00401-006-0073-9.

88. Mishra, T., Goel, N. A., & Goel, A. H. (2014). Primary paraganglioma of the spine: A clinicopathological study of eight cases. Journal of Craniovertebral Junction & Spine, 5(1), 20–24. https://doi.org/10.4103/0974-8237.135211.

89. Molloy, Patricia T., et al. “Central Nervous System Medulloepithelioma: a Series of Eight Cases Including Two Arising in the Pons in: Journal of Neurosurgery Volume 84 Issue 3 (1996).” Journal of Neurosurgery, Journal of Neurosurgery Publishing Group, 29 Oct. 2018, thejns.org/view/journals/j-neurosurg/84/3/article-p430.xml.

90. Muzio, Bruno Di, and Rohit Sharma. “1p19q Codeletion: Radiology Reference Article.” *Radiopaedia Blog RSS*, radiopaedia.org/articles/1p19q-codeletion.

91. Nambirajan, A., Sharma, M. C., & Rajeshwari, M. (2016). A Comparative Immunohistochemical Study of in the Diagnosis of Ependymomas, 00(00), 1–8.

92. Nguyen, Ha Son, et al. “Subependymal Giant Cell Astrocytoma: A Surveillance, Epidemiology, and End Results Program-Based Analysis from 2004 to 2013.” World Neurosurgery, U.S. National Library of Medicine, 30 June 2018, www.ncbi.nlm.nih.gov/pubmed/29966782.

93. Ohgaki, H., Eibl, R. H., Reichel, M. B., Mariani, L., Petersen, I., Höll, T., … Gehring, M. (1993). Mutations of the p53 tumor suppressor gene in neoplasms of the human nervous system. Molecular Carcinogenesis, 8(2), 74–80. https://doi.org/10.1002/mc.2940080203.

94. Okamatsu, Chizuko, et al. “Clinicopathological Characteristics of Ganglioneuroma and Ganglioneuroblastoma: A Report from the CCG and COG.” Pediatric Blood & Cancer, John Wiley & Sons, Ltd, 15 June 2009, onlinelibrary.wiley.com/doi/full/10.1002/pbc.22106.

95. Olar, Adriana, and Kenneth D Aldape. “Using the Molecular Classification of Glioblastoma to Inform Personalized Treatment.” *The Journal of Pathology*, U.S. National Library of Medicine, Jan. 2014, www.ncbi.nlm.nih.gov/pmc/articles/PMC4138801/.

96. Olig2 and CD99 are useful negative markers for the diagnosis of brain tumors. Clinical Neuropathology, 27(05), 118–128. https://doi.org/10.5414/npp27118.

97. Oslobanu, A., and Cluj-Napoca. “Anatomic Locations in High Grade Glioma.” Romanian Neurosurgery , 2015, www.degruyter.com/downloadpdf/j/romneu.2015.29.issue-3/romneu-2015-0036/romneu-2015-0036.pdf.

98. Pathack, Manish. “Boruta Feature Selection in R.” *DataCamp Community*, DataCamp, 7 Mar. 2018, www.datacamp.com/community/tutorials/feature-selection-R-boruta.

99. Pekmezci, M., Villanueva-Meyer, J. E., Goode, B., Van Ziffle, J., Onodera, C., Grenert, J. P., … Solomon, D. A. (2018). The genetic landscape of ganglioglioma. Acta Neuropathologica Communications, 6.

100. Perkins, Stephanie M., et al. “Patterns of Care and Outcomes of Patients with Pleomorphic Xanthoastrocytoma: a SEER Analysis.” SpringerLink, Springer US, 28 July 2012, link.springer.com/article/10.1007/s11060-012-0939-8.

101. Perry A, Brat DJ. Practical surgical neuropathology: a diagnostic approach. Philadelphia, PA: Churchill Livingstone Elsevier; 2018

102. Perry, A., Burton, S. S., Fuller, G. N., Robinson, C. A., Palmer, C. A., Resch, L., … Rosenblum, M. K. (2010). Oligodendroglial neoplasms with ganglioglioma-like maturation: A diagnostic pitfall. Acta Neuropathologica, 120(2), 237–252. https://doi.org/10.1007/s00401-010-0695-9.

103. Pisapia, David J. “Cellular and Molecular Origins of Adult Infiltrating Gliomas.” *The Updated World Health Organization Glioma Classification*, Dec. 2017, www.archivesofpathology.org/doi/pdf/10.5858/arpa.2016-0493-RA.

104. Poulen, G., Gozé, C., Rigau, V., & Duffau, H. (2018). Huge heterogeneity in survival in a subset of adult patients with resected, wild-type isocitrate dehydrogenase status, WHO grade II astrocytomas. Journal of Neurosurgery, 1–10. https://doi.org/10.3171/2017.10.jns171825.

105. Preusser, M., Laggner, U., Haberler, C., Heinzl, H., Budka, H., & Hainfellner, J. A. (2006). Comparative analysis of NeuN immunoreactivity in primary brain tumours: Conclusions for rational use in diagnostic histopathology. Histopathology, 48.

106. Puhan, M. A., Chandra, D., Mosenifar, Z., Ries, A., Make, B., Hansel, N. N., … Centre, H. (2017). HHS Public Access, 37

107. Reuss, D. E., Sahm, F., Schrimpf, D., Wiestler, B., Capper, D., Koelsche, C., … von Deimling, A. (2015). ATRX and IDH1-R132H immunohistochemistry with subsequent copy number analysis and IDH sequencing as a basis for an “integrated” diagnostic approach for adult astrocytoma, oligodendroglioma and glioblastoma. Acta Neuropathologica, 129.

108. Rheinboldt, Matt, et al. “Acute Presentation of Lhermitte-Duclos Disease in Adult Patient in Association with Cowden Syndrome.” Https://Appliedradiology.com/Articles/Acute-Presentation-of-Lhermitte-Duclos-Disease-in-an-Adult-Patient-in-Association-with-Cowden-Syndrome, Applied Radiology, Aug. 2016.

109. Rigau, Valérie, et al. “French Brain Tumor DataBase: 5-Year Histological Results on 25 756 Cases.” Brain Pathology, John Wiley & Sons, Ltd (10.1111), 25 July 2011, onlinelibrary.wiley.com/doi/full/10.1111/j.1750-3639.2011.00491.x.

110. Rodriguez, F. J., Perry, A., Rosenblum, M. K., Krawitz, S., Cohen, K. J., Lin, D., … Burger, P. C. (2012). Disseminated oligodendroglial-like leptomeningeal tumor of childhood: a distinctive clinicopathologic entity. Acta Neuropathologica, 124(5), 627–641.

111. Sang, K., & Gheeyoung, L. (2013). Immunohistochemical Classification of Primary and Secondary Glioblastomas, 541–548.

https://doi.org/10.1007/s00401-012-1037-x.

112. Scharnhorst, D. W., Shih, C.-S., Dabiri, S., Du, E., Ellison, D. W., Baker, J. A., … Li, R. (2015). Epithelioid Glioblastomas and Anaplastic Epithelioid Pleomorphic Xanthoastrocytomas-Same Entity or First Cousins? Brain Pathology, 26(2), 215–223. https://doi.org/10.1111/bpa.12295.

113. Schlamann, Annika, et al. “An Individual Patient Data Meta-Analysis on Characteristics and Outcome of Patients with Papillary Glioneuronal Tumor, Rosette Glioneuronal Tumor with Neuropil-like Islands and Rosette Forming Glioneuronal Tumor of the Fourth Ventricle.” PloS One, Public Library of Science, 3 July 2014, www.ncbi.nlm.nih.gov/pmc/articles/PMC4084640/.

114. Schwab, D. E., Lepski, G., Borchers, C., Trautmann, K., Paulsen, F., & Schittenhelm, J. (2018). Immunohistochemical comparative analysis of GFAP, MAP – 2, NOGO – A, OLIG – 2 and WT – 1 expression in WHO 2016 classified neuroepithelial tumours and their prognostic value. Pathology Research and Practice, 214(1), 15–24. https://doi.org/10.1016/j.prp.2017.12.009.

115. Seno, T., Kawaguchi, T., Yamahara, T., Sakurai, Y., Oishi, T., Inagaki, T., … Kawamoto, K. (2008). An immunohistochemical and electron microscopic study of atypical teratoid/rhabdoid tumor. Brain Tumor Pathology, 25(2), 79–83. https://doi.org/10.1007/s10014-008-0236-6.

116. Sethi, Divya, et al. "Choroid Plexus Papilloma." Asian Journal of Neurosurgery, Medknow Publications & Media Pvt Ltd, 2017, www.ncbi.nlm.nih.gov/pmc/articles/PMC5379790/.

117. Sharma, M. C., Ralte, A. M., Arora, R., Santosh, V., Shankar, S. K., & Sarkar, C. (2004). Subependymal giant cell astrocytoma: a clinicopathological study of 23 cases with special emphasis on proliferative markers and expression of p53 and retinoblastoma gene proteins. Pathology, 36(2), 139–144. https://doi.org/10.1080/00313024100016719 75.

118. Son, E. I., Kim, I. M., Kim, D. W., Yim, M. Bin, Kang, Y. N., Lee, S. S., … Kim, S. P. (2003). Immunohistochemical analysis for histopathological subtypes in pediatric medulloblastomas. Pathology International, 53(2), 67–73. https://doi.org/10.1046/j.1440-1827.2003.01444.x.

119. Sol, S. (2018). Clinicopathological and Molecular Analysis on Papillary and Rosette-Forming Glioneuronal Tumours, (March), 2–3. https://doi.org/10.13140/RG.2.2.16227.04644.

120. Solomon, D. A., Wood, M. D., Tihan, T., Bollen, A. W., Gupta, N., Phillips, J. J. J., & Perry, A. (2016). Diffuse Midline Gliomas with Histone H3-K27M Mutation: A Series of 47 Cases Assessing the Spectrum of Morphologic Variation and Associated Genetic Alterations. Brain Pathology, 26(5), 569–580. https://doi.org/10.1111/bpa.12336.

121. Suri, V. S., Tatke, M., Singh, D., & Sharma, A. (2004). Histological spectrum of ependymomas and correlation of p53 and Ki-67 expression with ependymoma grade and subtype. Indian Journal of Cancer, 41(2), 66–71. Retrieved from http://www.ncbi.nlm.nih.gov/pubmed/15318011.

122. Theeler, B. J., Yung, W. K. A., Fuller, G. N., & De Groot, J. F. (2012). Moving toward molecular classification of diffuse gliomas in adults. Neurology, 79(18), 1917–1926. https://doi.org/10.1212/WNL.0b013e318271f7cb.

123. Thotakura, M., Tirumalasetti, N., & Krishna, R. (2014). Role of Ki-67 labeling index as an adjunct to the histopathological diagnosis and grading of astrocytomas. J Cancer Res Ther, 10(3), 641–645. https://doi.org/10.4103/0973-1482.139154.

124. Tsumanuma, I, et al. "The Analysis of p53 Tumor Suppressor Gene in Pineal Parenchymal Tumors." *Noshuyo Byori = Brain Tumor Pathology*, U.S. National Library of Medicine, Mar. 1995, www.ncbi.nlm.nih.gov/pubmed/7795728.

125. VandenBerg, Scott R. "Desmoplastic Infantile Ganglioglioma and Desmoplastic Cerebral Astrocytoma of Infancy." Brain Pathology, John Wiley & Sons, Ltd (10.1111), 28 Jan. 2008, onlinelibrary.wiley.com/doi/epdf/10.1111/j.1750-3639.1993.tb00754.x.

126. Venneti, S., Le, P., Martinez, D., Eaton, K. W., Shyam, N., Jordan-Sciutto, K. L., … Judkins, A. R. (2011). P16INK4A and p14ARF tumor suppressor pathways are deregulated in malignant rhabdoid tumors. Journal of Neuropathology and Experimental Neurology, 70(7), 596–609. https://doi.org/10.1097/NEN.0b013e31822146ca.

127. Wani, Khalida, et al. “Histological Predictors of Outcome in Ependymoma Are Dependent on Anatomic Site Within the Central Nervous System.” Brain Pathology, John Wiley & Sons, Ltd (10.1111), 28 Mar. 2013, onlinelibrary.wiley.com/doi/pdf/10.1111/bpa.12050.

128. Wu, Jing, et al. “Biology and Management of Ependymomas.” Neuro-Oncology, Oxford University Press, July 2016, www.ncbi.nlm.nih.gov/pmc/articles/PMC4896548/.

129. Yang, Chenlong, et al. “Histopathological, Molecular, Clinical and Radiological Characterization of Rosette-Forming Glioneuronal Tumor in the Central Nervous System.” Oncotarget, Impact Journals LLC, 24 Nov. 2017, www.ncbi.nlm.nih.gov/pmc/articles/PMC5752512/.

130. Yang, M., Chen, X., Wang, N., Zhu, K., Hu, Y. Z., Zhao, Y., … Tang, H. F. (2014). Primary atypical teratoid/rhabdoid tumor of central nervous system in children: A clinicopathological analysis and review of literature in China. International Journal of Clinical and Experimental Pathology, 7(5), 2411–2420.

131. Yang, Z., Yan, F., Meng, L., Ao, Q., & Zhu, P. (2013). Clinicopathological and immunohistochemical features of pilomyxoid astrocytoma: A report of six cases. Chinese-German Journal of Clinical Oncology, 12(9), 423–426. https://doi.org/10.1007/s10330-013-1190-2.

132. Yobero, Czar. “Determining Creditworthiness for Loan Applications Using C5.0 Decision Trees.” *RPubs*, Rstudio, 7 Aug. 2018, rpubs.com/cyobero/C50.

133. You, H., Kim, Y. I., Im, S. Y., Suh-Kim, H., Paek, S. H., Park, S.-H., … Jung, H.-W. (2005). Immunohistochemical study of central neurocytoma, subependymoma, and

subependymal giant cell astrocytoma. Journal of Neuro-Oncology, 74(1), 1–8. https://doi.org/10.1007/s11060-004-2354-2.

134. Zakrzewska, M., Szybka, M., Biernat, W., Papierz, T., Rieske, P., Liberski, P. P., & Zakrzewski, K. (2009). Prevalence of mutated TP53 on cDNA (but not on DNA template) in pleomorphic xanthoastrocytoma with positive TP53 immunohistochemistry. Cancer Genetics and Cytogenetics, 193.

135. Zhikrivetskaya, S. O., Snezhkina, A. V., Zaretsky, A. R., Alekseev, B. Y., Pokrovsky, A. V., Golovyuk, A. L., … Kudryavtseva, A. V. (2017). Molecular markers of paragangliomas/pheochromocytomas. Oncotarget, 8(15), 25756–25782. https://doi.org/10.18632/oncotarget.15201.